Available online at www.sciencedirect.com

ScienceDirect

Procedia Structural Integrity 24 (2019) 612–624

Structural Integrity Procedia

www.elsevier.com/locate/procedia

AIAS 2019 International Conference on Stress Analysis

Numerical evaluation of internal heat generation of roller coaster polyurethane wheels

Claudio Braccesi[a],Filippo Cianetti[a] *, Alberto Ferri[b]

[a]*Università degli Studi di Perugia, Dipartimento di Ingegneria, Via Goffredo Duranti, 67, 06125 Perugia*
[b]*Antonio Zamperla S.p.A., Via Monte Grappa, 15, 36077 Altavilla Vicentina (VI)*

Abstract

Nowadays, polymeric materials are used in a wide range of applications such as building and construction, transportation, machinery, electronics. In this paper, the polyurethane, used in roller coaster wheels, was considered and analyzed. The main aim of the research activity is to understand the damaging mechanisms that characterize the material. Experimental results show that the polyurethane can be degraded not only by mechanical fatigue but also by thermal degradation mechanisms which depend on the temperature, caused by both weather conditions and internal heat generation (loss of energy as heat). In particular, the relationship between velocity and intensity of applied loads and the amount of lost energy (lost as heat) was analyzed, with the aim to develop, within a generic finite element analysis code, a methodology to estimate the temperature distribution in a roller coaster wheel, by knowing its load and velocity time history

Keywords: polyurethane; rollercoaster wheels; self-heating; thermal analysis; finite element analysis

1. Introduction

This paper analyzes the problem of assessing the temperature raising of coating polymeric material of the wheels used for rollercoaster cars (Figure 1).

* Corresponding author. Tel.: +39 075 5853728; fax: +39 075 5853703.
E-mail address: filippo.cianetti@unipg.it

10.1016/j.prostr.2020.02.054

It is part of a wider research scenario that aims to identify, to simulate and experimentally verify the damage conditions of roller coaster (RC) and in particular of wheels, a component very important for the RC behavior both in terms of functionality and of safety [Braccesi et al. (2015), Braccesi et al. (2018)].

The rollercoaster wheels have a metal core and are coated with polyurethane (Figure 1), a material characterized by viscoelastic behavior and, consequently, by an hysteretic behavior in terms of stress/strain relations. This material is used for its outstanding ability to dissipate energy, to damp vibrations and to absorb shocks.

One of the main causes of damage of polyurethane is certainly the temperature that is reached during operating conditions and its variations. This is the reason that addressed the authors to the evaluation of temperature evolution of wheels during the operating conditions.

The scientific contribution (applied science) of the present research is the proposal of a simulation methodology more simple than the hypothetic canonic one, that allows the designer to obtain a reliable evaluation of the polyurethanic wheels to be chosen. To this aim in this paper the authors have proposed a methodology of temperature assessment by using finite element modeling and simulation.

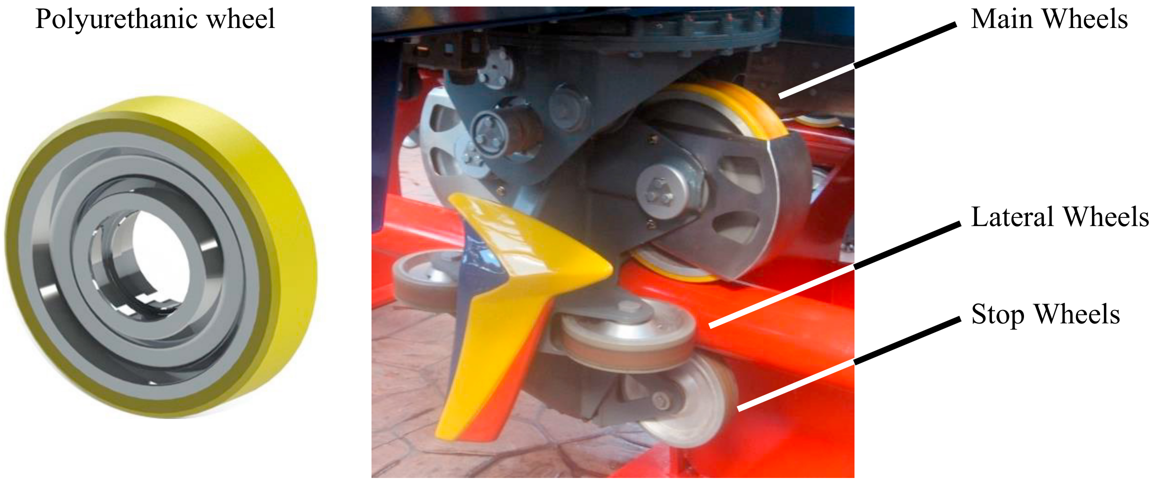

Fig. 1. Example of Polyurethanic wheel and of a rollercoaster wheels group

The self-heating caused by load time history and material internal dissipation is a complex phenomena; the literature confirms that can not be directly simulated by commercial finite element codes [Gopalakrishna et al. (1998), de Cazenove et al. (2012)], neither by the so-called coupled-field analysis, that couples mechanical (hysteresis) and thermal (temperature distribution evaluation) simulation. However, hypothesizing to have a finite element code with this potential, the direct coupling between thermal and structural fields would result in prohibitive computational costs. This has led the authors to develop a technique that, although bases on simplifying assumptions, has proven to efficiently obtain the desired aims, as efficient in terms of results and fast in terms of computational times.

In Section 2 the main characteristics and the main forms of damage of polymeric materials are described, with special attention to the polyurethane. In Section 3 the main constitutive models that allow the numerical modeling of polymeric materials are shown. In Section 4 the principal idea of the paper, that is the technique for the evaluation of the dissipated power in the form of heat, is illustrated. In section 5 this approach is applied to a rotating wheel and then used to analyze a test case of industrial interest. A rollercoaster is analyzed and the proposed method is used to compare and critically analyze three wheel solutions.

2. Polymeric materials

The word polymer, which literally means "many parts", indicates a macromolecule, which is a molecule with an high molecular weight, which consists of several parts or units, chemically linked to each other, called monomers [Kalpakjian et al. (2006), Gogos et al. (2006), Ebewele (2000)].

From the point of view of its mechanical characteristics, the polymer called polyurethane has a behavior that depends on both temperature and load rate; it is characterized by the phenomenon of creep (increasing deformation over time when subjected to a constant load), by the phenomenon of stress relaxation (reduction in time of the stress at a constant imposed deformation) and by the energy loss due to hysteresis. That is, by applying a loading and unloading cycle to a polyurethane component, it is observed, on the force-displacement environment, a loading curve different from that of unloading one and the observed area physically represents the energy dissipated in the form heat in the loading and unloading cycle.

Among the possible causes of damage of the polyurethane, it is possible to consider: the mechanical fatigue, the photo-degradation and thermal degradation [Bakirani et al. (1992), Mead (1996), Beyler et al. (2008), Zeus Ind. Prod. (2005)]. The latter is a deterioration associated with an excessive heating process, which thus is connected with the temperature reached by the polymer. As a result of this damage phenomenon occurs the formation of cracks, reduction of ductility, chalking, color change or cracking. These are the same phenomena recorded on the polyurethane coating of roller coaster wheels, and therefore it is possible to infer that the thermal degradation is the form of damage that affects the wheels.

3. Material constitutive models

Polymeric materials have viscoelastic behavior; viscoelasticity is the property of materials that exhibits both elastic and viscous characteristics. In particular, polyurethane have not a classic linear elastic behavior but a non-linear elastic one called hyper-elasticity.

To model the hyper-elastic behavior many models have been proposed; each of them provides its own expression of strain energy density function (or elastic potential function) per unit undeformed volume, W. The most popular models are: Arruda-Boyce model, Gent model, Mooney-Rivlin model, Odgen model, Yeoh model [Ansys (2012), Brinson et al. (2008), Dal et al. (2009), Briody et al. (2012)].

To analyze viscoelastic behavior, lots of constitutive models have been proposed: Maxwell model, generalized Maxwell model, Kelvin-Voigt model, generalized Kelvin-Voigt, Zener, generalized Zener [Ansys (2012), Brinson et al. (2008), Dal et al. (2009), Briody et al. (2012)]. All these models are characterized by a constitutive equation and can be constructed using springs and dampers in series and parallel combinations. For example, for generalized Maxwell model the constitutive equation can be written as:

$$\sigma = \int_0^t 2G(t-\tau)\frac{de}{d\tau}d\tau + I\int_0^t 2K(t-\tau)\frac{d\Delta}{d\tau}d\tau \tag{1}$$

where $\boldsymbol{\sigma}$ is the Cauchy stress, $\boldsymbol{e}$ is the deviatoric strain, Δ is the volumetric strain, $\boldsymbol{\tau}$ is the past time, $\boldsymbol{I}$ is the identity tensor, $\boldsymbol{G} = \boldsymbol{G}(\boldsymbol{t})$ is the shear modulus expressed by the Prony series (Equation 2) and $\boldsymbol{K} = \boldsymbol{K}(\boldsymbol{t})$ is the bulk-relaxation modulus (Equation 3).

$$G(t) = G_0\left[\alpha_\infty^G + \sum_{i=1}^{n_G} \alpha_i^G e^{-\frac{t}{\tau_i^G}}\right] \tag{2}$$

$$K(t) = K_0\left[\alpha_\infty^K + \sum_{i=1}^{n_K} \alpha_i^K e^{-\frac{t}{\tau_i^K}}\right] \tag{3}$$

In Equations 2 and 3 superscripts shows belonging to shear or bulk modulus and subscript indices the number of series component. $\boldsymbol{G_0}$ and $\boldsymbol{K_0}$ are the moduli at $\boldsymbol{t}$ = 0, $\boldsymbol{n_G}$ and $\boldsymbol{n_K}$ are the number of Prony terms, $\boldsymbol{\tau_i} = \boldsymbol{\mu_i}/\boldsymbol{E_i}$ is called relaxation time constant, $\boldsymbol{\alpha_i}$ is equal to $\frac{G_i}{G_0}$ and $\boldsymbol{\alpha_\infty}$ could be simply calculated by $\boldsymbol{t}$ equal to zero.

If a single degree of freedom (sdof) is considered, constituted by a spring (elastic element) and a damper (viscous element) connected to each other in parallel and without mass, its equation of motion is [Paez et al. (2009)]:

$$c\dot{x}(t) + kx(t) = f(t) \tag{4}$$

where $x(t)$ represents system motion with respect to the position of stable equilibrium, $\dot{x}(t)$ is the velocity that is the first derivative of displacement with respect to time, $f(t)$ is the external force applied to the system, k is the stiffness of the spring and c is the viscous damping parameter of the damper. Applying a force to the system and displaying the relation force-displacement, a hysteretic cycle is observable.

This area, from a mathematical point of view [Paez et al. (2009)], can be expressed by Equation (5).

$$E = \int f(t)dx \tag{5}$$

In the previous equation, the infinitesimal variation of displacement dx can be rewritten as:

$$dx = \dot{x}(t)dt \tag{6}$$

By substituting Equation (6) into (5) it can be obtained the following:

$$E = \int_0^T f(t) \cdot \dot{x}(t)dt \tag{7}$$

where T is the integration time in which the energy loss is evaluated and the product $f(t) \cdot \dot{x}(t)$ represents the power, whose integration in time, therefore, is the energy loss as heat.

The idea born from this result is the possibility to extend this method to a generic finite element model, going to assess the power from the data which typically a FEM code provides. Thus passing from a sdof system to a FE model with elements having m nodes and n dof/node (and thus $m \times n$ degrees of freedom for each element), to evaluate the power at the time instant r-th for the i-th element coincides with to perform the scalar product:

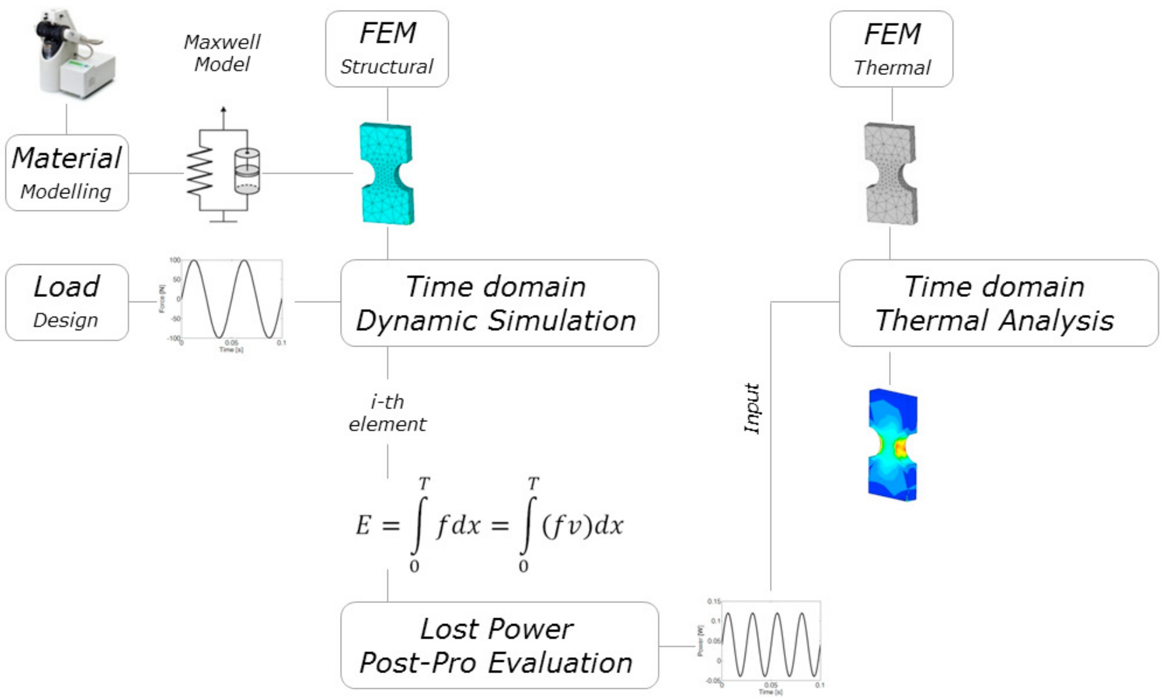

Fig 2. Flow-chart of the proposed procedure

$$W(t_r)_i = \{f(t_r)\}_i \times \{v(t_r)\}_i \quad (8)$$

where $\{f(t_r)\}_i$, of size (1, $m \times n$), represents the vector of nodal forces of the i-th element at r-th instant, $\{v(t_r)\}_i$, of size ($m \times n$, 1), is the vector of nodal velocity of the i-th element at r-th instant and $W(t_r)_i$ represents the value of the power loss by the element i-th at r-th instant.

This operation, repeated for each element of the model and for each time instant, would allow to obtain, for each element, a time history of power $\{W(t)\}_i$ that represents the heat power loss by the material, consequence of a mechanical deformation due to the application of external loads.

The technique, proposed by the authors, for the assessment of the resulting temperature due to the internal dissipation of the material, bases on to decouple the two phases: mechanical analysis and thermal analysis. As regards the first phase, this methodology bases on the realization of the structural finite element model of a generic component, in the application of dynamic loads and in the evaluation, in post processing, of the time histories of power loss of each element, by using the technique described by (8). At this point, having available the thermal power, a thermal analysis is needed by realizing the thermal finite element model of the same component and performing a time domain transient thermal analysis having power loss time history (previously assessed) as input, and defining appropriate initial and boundary conditions.

This developed procedure is easily implementable in a finite element code, as shown in Figure 2. It needs to generate the twin thermal model of the structural one, in which the material exhibits the correct thermal properties of density, specific heat and thermal conductivity, and to perform a thermal analysis with the time history of power loss as input and obtaining as a result the temperature distribution.

The input power loss time history are obtainable by the (9):

$$\{q^*(t)\} = \frac{\{W(t)\}_i}{V_i} \quad (9)$$

where $\{q^*(t)\}$ represents the heat internally generated per unit of time and volume from the generic i–th V_i volume.

4. Roller coaster wheels simulation

The main aim of the present work, however, is to develop a finite element simulation (FEA) technique to obtain the thermal field of a wheel (Figure 1) belonging to a roller coaster car that runs on a generic roller coaster track, loaded by a variable load and subjected to a variable translational and rotational velocity. These inputs are assumed to be known and obtainable by a multibody simulation (MBS) [Braccesi et al. (2015), Braccesi et al. (2018), Zheng et al. (2017)] or by experimental measures. The methodology presented in Section 5 could be easily applied to a wheel if to perform a dynamic analysis was easily. This means to perform a simulation of the same wheel which rolls on a track as long as the entire track, for example of 400 m length, which is subjected to a variable speed and to a variable load, applied to the wheel center. To perform this kind of simulation is, in practice, impossible.

For these reasons, the authors have morphed the previous proposed methodology to the case of the roller coaster wheel by simplifying to the maximum the phase of dynamic analysis and results post processing in order to simply conduct the thermal transient analysis. A synthetic flow chart of the proposed procedure useful to approach RC wheels analysis is shown in Figure 3.

The wheel is a more complex component than that represented in flow chart of figure 2. The load is transferred by the wheel centre to the periphery (in this case to the polyurethane) in a cyclic way, with a period dependent both from the speed and from the load. The load itself modify wheel radius and determines the variation of the angular velocity with respect to the ideal one that would be achieved with a rigid wheel. The variation of the load, in addition to produce diameter variations, urges variable circular sectors of the wheel, much broader as much as the load is high. It can be said, therefore, that the load condition and, therefore, also the amount of heat, internally dissipated, are function both of the speed and of the load value.

First difficulty that must be addressed is the application modality of the load and, then, the simulation of the real operating conditions of the wheel which, in addition to be loaded by a variable load, is in contact and in roto-translational motion on a tubular rail characterized by double curvature.

In order to eliminate the rigid motions of the wheel, first result and dictates of the proposed procedure is to analyze the wheel keeping it stopped with respect its rotational axis, and loading and rotating the rail around it, by applying a rotational velocity congruent with the translational velocity of the wheel itself (Figure 4).

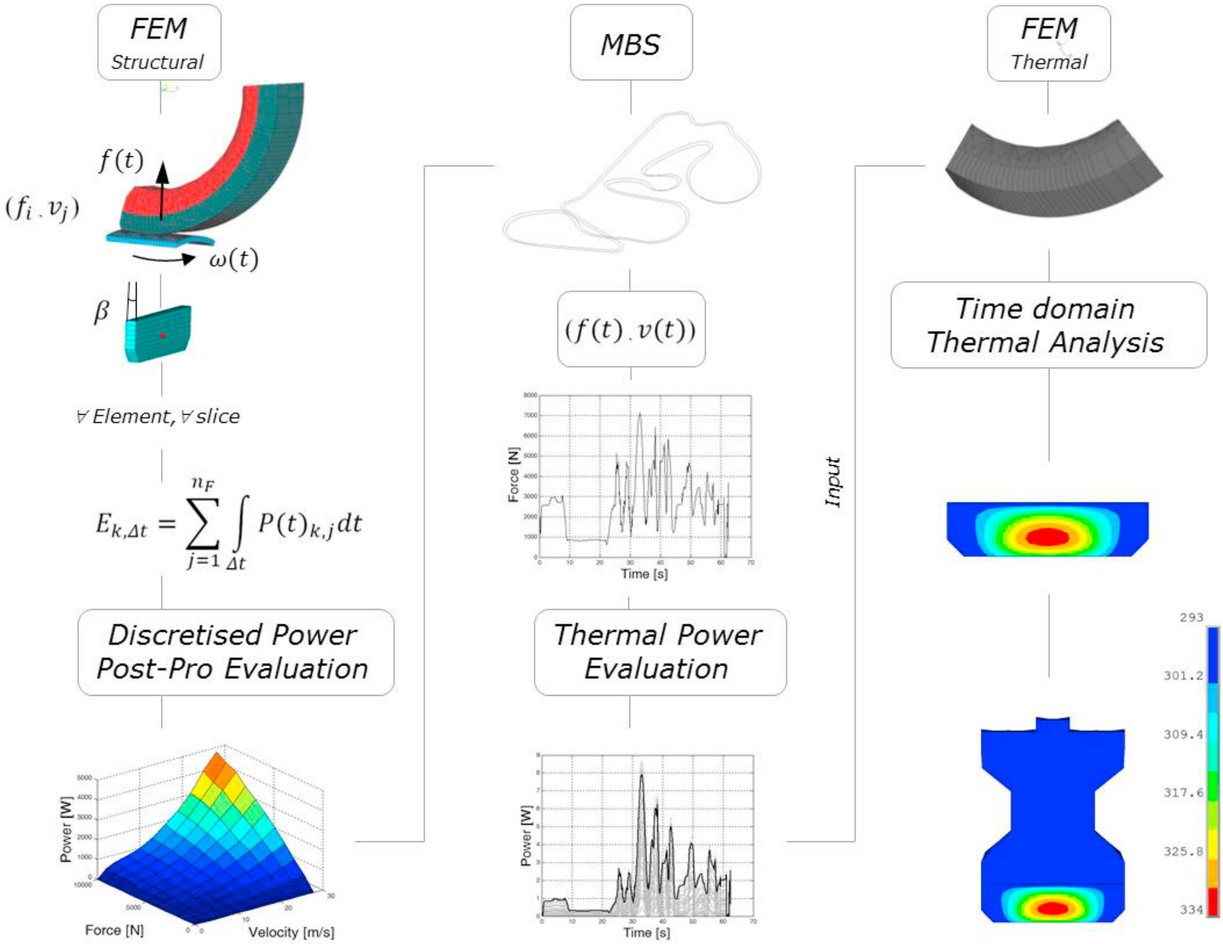

Fig. 3. Flow-chart of the proposed procedure applied to RC wheels analysis

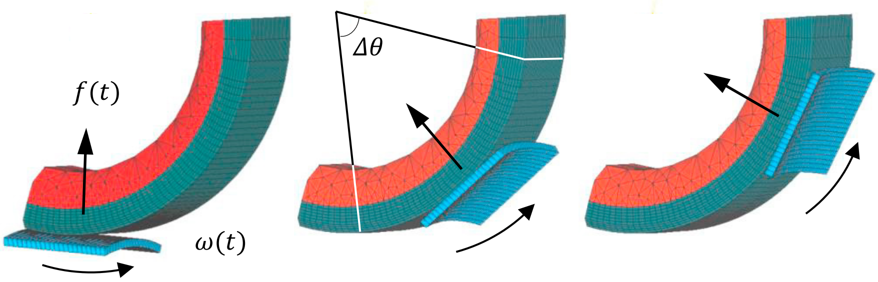

Figure 4. Proposed Wheel/Track FE model. The wheel is stopped with respect its rotational axis and the rail loads it and rotates around it (from left to right in the figure sequence) with a rotational velocity congruent with the translational velocity of the wheel itself.

From the methodological point of view, the subsequent adopted choice, for the simplification of the procedure, has been to hypothesize that the recovery of the power loss time history, i.e. of the time histories of forces and nodal velocities of each element, could be discretized and evaluated regardless of the real time history of these variables in a range of operating values (having as parameters the translational speed and the wheel center load) congruent to the real operation of the vehicle (i.e. assuming as range extremes the maximum and minimum values of load and speed obtained from multibody simulation)

This means to evaluate the real operating condition in terms of stress, strain and, especially, heat for assigned pairs of values of load f_i and speed v_j with $i = 1,\ldots,n$ and $j = 1,\ldots,m$, assuming these as constants for each simulation of the $m \times n$ expected. Each of $m \times n$ dynamic analysis is a simulation of the wheel rolling by applying a pair of values (f_i, v_j), simulating a complete wheel turn and analyzing the results. This allows to hypothesize to recover the power loss time history of the elements by interpolating the true stories of translational speed and load and the results obtained in the discretized variables environment described before.

Another aspect that should be noted is that considering a complete wheel revolution, the load application, in terms of strain and stress and, then, lost power constantly involves only an angular sector $\Delta\theta_i$, measured respect to a reference system that does not change its orientation and that rigidly moves itself with the center wheel; this sector has an amplitude which is function of the load value f_i and that is also evaluable by means of a trivial static analysis. It is then sufficient to analyze the motion of the wheel and its stress state condition exclusively for a circumferential extension equal to the width of this sector (Figure 4), minimizing the burden of computation and the duration of the single ij-th dynamic analysis.

Further observation is that, considering each of the radial sections of the previously identified sector $\Delta\theta_i$ and observing for each element and for each node the time history of the above mentioned parameters (i.e. radial deformation), it is observable that each of the time histories is a copy of the next or of the previous section (elements or nodes) one and characterized by a time shift proportional to the rolling speed ω of the wheel (hence, to the forward one too) and of the relative angular measures, evaluated with respect to the considered reference section. In presence of regular mesh and of constant circumferential angular dimensions of the elements (i.e. equal to β) the time shift, associated with each section can be quantified by (10):

$$\delta t = \frac{\beta}{\omega} \tag{10}$$

with β expressed in radiant.

In this way it has come to the conclusion that it is necessary to monitor only a section of elements belonging to the sector $\Delta\theta_i$ leaving to the post processing stage the task of recovering for the generic force f_i and velocity v_j the time history of the thermal power dissipated by this section and by all the others through time shifts applied to the time histories extracted from this single section. Even if $\Delta\theta_i$ angle is not a fixed value because is function of force f_i and velocity v_j typical values adopted by authors in this research activity vary between 90 and 100 degrees.

The described methodology is thus based on considering for each pair of parameters (force, speed) a constant value of the dissipated thermal power for each ring. To obtain this value, it is necessary to identify for each dynamic analysis, and for each pair (f_i, v_j), the time interval Δt in which the radial row of elements of the considered ring exerts its

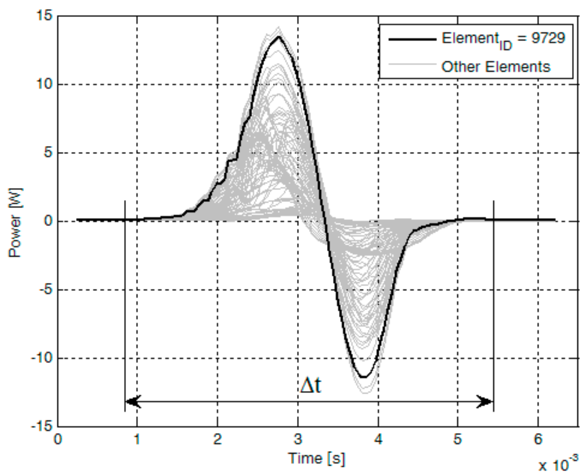

Fig. 5. Example of Polyurethanic wheel and of a rollercoaster wheels group

influence from the point of view of energy dissipation (Figure 5). In this time interval, however, there is not only the contribution of the section considered but also that of n_F upstream and downstream sections to be determined. The number n_F of sections is obtainable by moving forward and backward in time, with δt increments, the obtained power curves and verifying whether they continue to fall back within the range Δt. By calling n_F the total number of energy-contributing sections, the energy dissipated in heat from each ring k of elements in this range $E_{k,\Delta t}$ is obtained by applying (11):

$$E_{k,\Delta t} = \sum_{j=1}^{n_F} \int_{\Delta t} P(t)_{k,j} dt \tag{11}$$

with j the index of the n_F considered sections, with $P(t)_{k,j}$ the power associated with the k-th element (ring) of the j-th section at instant t.

By indicating with T the time that the wheel takes to make a turn, it is possible to evaluate the energy dissipated in a round from each ring of elements by (12).

$$E_{round,k} = E_{k,\Delta t} \frac{T}{\Delta t} \tag{12}$$

The power to be attributed to the k-th ring is obtained by dividing the previously calculated energy (11) for the time interval at which it has been evaluated (12).

$$P_k = \frac{E_{round,k}}{T} \tag{13}$$

The equation (13) provides the power dissipated by each ring of elements when the wheel is working with the considered pair of values of force and speed.

Repeating this procedure (analysis and post processing) to all arbitrarily selected pairs of force and speed, a map of dissipated power is obtainable, function of speed and force; by this map it is possible to interpolate the real pairs of values obtained at each instant of the multibody simulation (MBS) and, then, to recover in post-processing the time histories of power to apply to each ring and then to each element.

The final step of the procedure is the realization of the Thermal FE model of the wheel (twin of the previous one in which it is enough to replace the structural element type with the thermal one) and to perform a transient thermal analysis having as input the time histories of dissipated power, previously evaluated, divided by the volume (9) of the ring being considered. As a result, the evolution of the temperature distribution of the wheel is obtained when it is in the specific track.

The developed procedure was tested by analyzing a Roller Coaster called Twister Coaster made by Zamperla S.p.A. (Italian factory of Altavilla Vicentina, Italy) and installed at Istanbul, Turkey, in 2014.

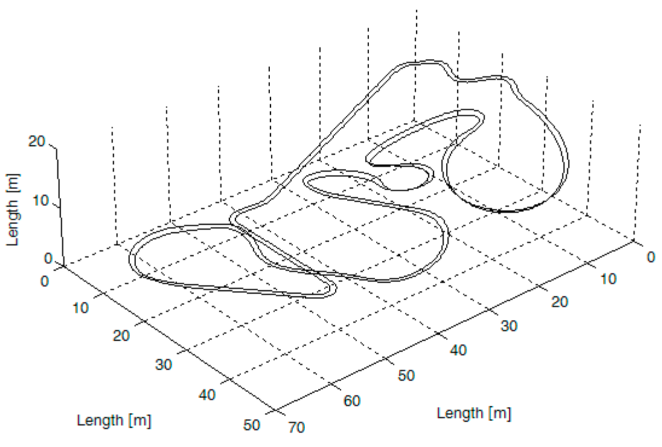

Fig. 6. Roller coaster test case. Track representation

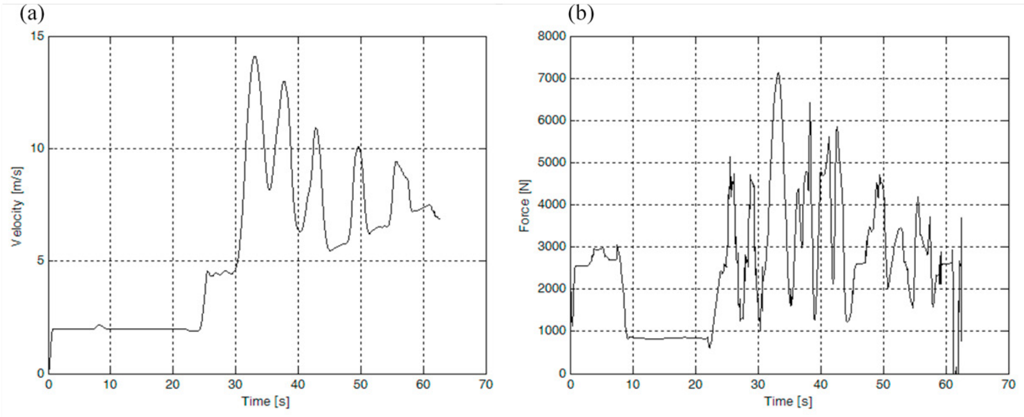

Fig. 7. Example of Polyurethanic wheel and of a rollercoaster wheels group

Table 1: Material. Prony series coefficients

α_i^G [no units]	τ_i^G [s]
0.532	$2.6 \cdot 10^{-5}$
0.034	0.007
0.072	0.009
0.016	0.0062
0.260	$2.6 \cdot 10^{-5}$

Table 2: Material. Coefficients of Mooney-Rivlin potential

Parameter	Value	Unit
C_{10}	21428571	[Pa]
C_{01}	0	[Pa]
d	$9.33 \cdot 10^{-9}$	[Pa^{-1}]

Table 3: Tested Wheels. Geometrical parameters

		Type A	Type B	Type B
D	[mm]	250	350	380
L	[mm]	60	90	90
s	[mm]	16	10	10

It is characterized by an overall length of 341 m, by a maximum travel speed of 14 m/s (Figure 6), by a duration of the single run of 63 s and by a maximum load value on the single wheel of 7120 N (Figure 7). The vehicle and wheel behavior has been simulated by a commercial multibody code (MSC.Adams/View) customized by authors to model generic vehicles and tracks [Braccesi et al. (2015), Braccesi et al. (2018)]. From the dynamic analysis, the time histories of force and speed at the center of the wheel were obtained in the local reference system (Figure 7).

The assessing technique of temperature distribution of a generic roller coaster wheel when a generic track is traveled has been applied to three different wheels that will be called "wheel A", "wheel B", and "wheel C" (Figure 8). The parameters of the material used to model the polyurethane are given in Table 1 and 2. Wheels outside diameter (D), width (L) and the peripheral polyurethane region thickness (s) are reported in Table 3. Wheel B has an outside

Table 4: Test case analyses. Discretized ranges of f_i, v_j for values of force and velocity

Force	[kN]	0.25	1	2	3	4	5	6	7	8	9	10
Velocity	[$^m/_s$]	2	4	7	10	13	16	19	22	25	28	

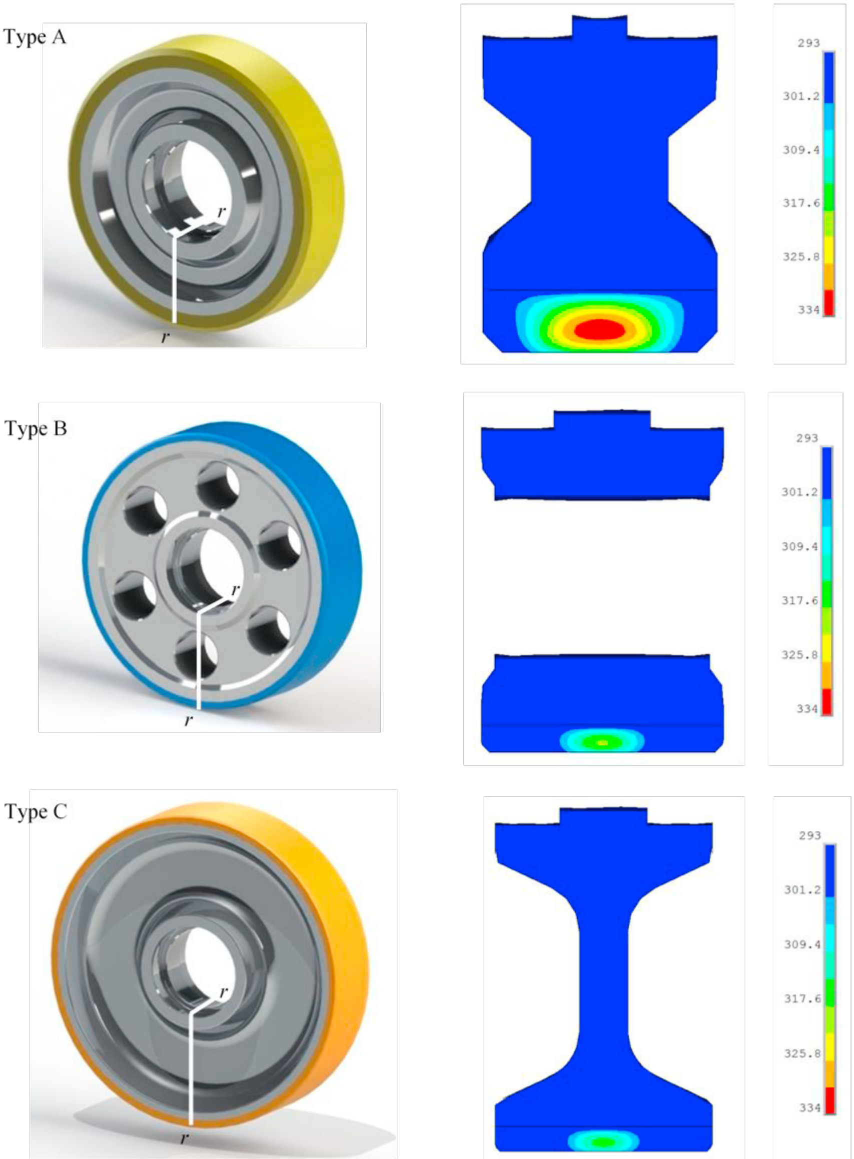

Fig. 8. Description of test wheels (left column) and results obtained in terms of temperature distribution [°K] at the end of the analyses on the lower sections (*r-r*) of the wheels by proposed analysis (right column)

diameter of 350 mm, width 90 mm and thickness of the polyurethane region of 10 mm. Wheel C has an outside diameter of 380 mm, width 90 mm and thickness of the polyurethane region of 10 mm.

The developed wheel models are shown in Figure 8 (left column). The wheel models are characterized by about 900.000 elements. The mesh is made by 8 nodes brick elements with 3 degrees of freedom per node. The circumferential dimension β of the mesh of polyurethane elements is 0.03 radiants (2 degrees). The arc that typically characterizes the stressed zone $\Delta\theta_i$ has magnitude between 20 and 40 degrees.

The tube has a circular hollow section with an outside radius of 140 mm and a thickness of 5 mm.

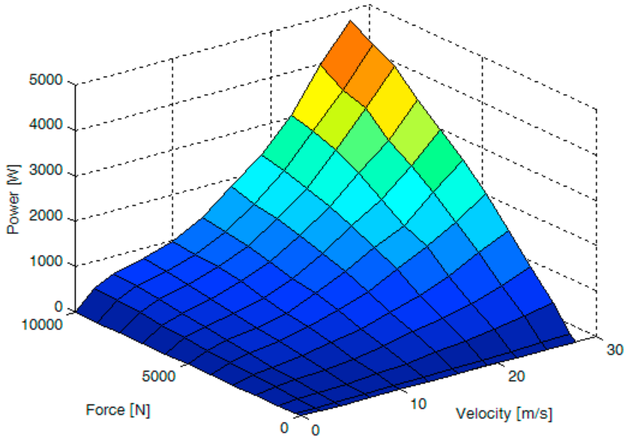

Fig. 9. Map of thermal power vs. wheel load and vehicle velocity - Wheel type A

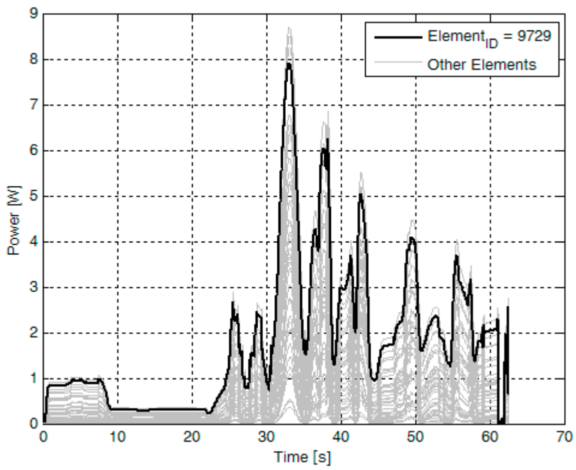

Fig. 10. Power time histories of the elements of the slice - Wheel type A

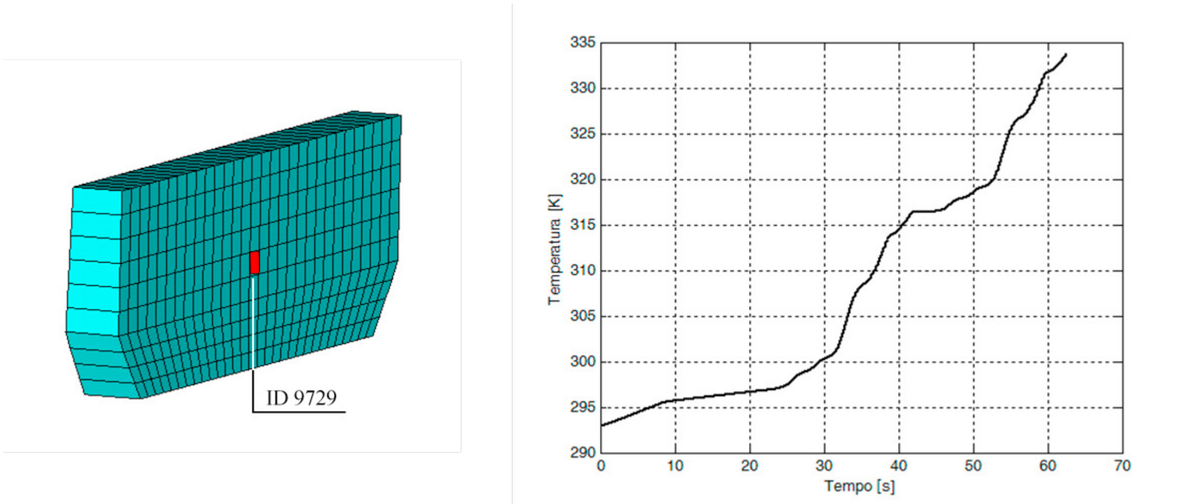

Fig. 11. Resulting time history for element ID 9729 – Wheel type A

Only the upper portion of the tube is modeled and simulated and the material used is steel with an elastic modulus of 2.1·1011 N/m^2 and a Poisson ratio of 0.3.

The speed/force ranges varies from 250 to 10000 N by 1000 N for force and from 2 to 28 m/s by 3 m/s for speed (Table 4). This means 110 dynamic analyses for each wheel model, each one characterized by computational times of 2 hours (220 hours total; this and other estimates are relative to a personal computer with Intel Core i7 processor CPU 980 3.33 GHz and 24 GB of RAM).

Obtained the power maps for each ring, in function of speed and force (Figure 9), and obtained the time histories of power per unitary volume (by a numerical code as Matlab) to be applied to each ring itself (Figure 10), the transient thermal analysis was carried out for each of the considered wheel models.

To accomplish each of these 3 analyses, it is necessary a computational time of 7 hours.

At the end of this procedure, the temperature time history or its distribution for each element are obtained. The temperature distributions are shown in right column of Figure 8 for the wheels A, B, C. The shown temperatures are expressed in Kelvin [K] and were obtained starting from an initial condition of Temperature of 293 K by imposing the convection boundary condition on the external surfaces with a convection coefficient h equal to 60 W/(m^{2}K) which simulates the heat exchange between the wheel and the air.

In these three images it is noted that the center of the wheel, made of aluminum, does not undergo temperature increase with respect to the initial condition, whereas the increase of the temperature of the polyurethane is sensitive and particularly marked in the center of that zone, where a maximum temperature of 333.7 K, 318.3 K and 315.4 K is recorded. Therefore, from this comparison, it is possible to infer that the C wheel is the best among the three analyzed solutions because it has the lowest increase in temperature and therefore the lowest value of damage.

There are no experimental tests and certified survey campaigns that can confirm this result, but the experience and summary evaluations conducted in situ by simple temperature measurements on their outer surface confirmed the same numerical quality trend, that is which were the most overheated wheels and the overheating order of magnitude.

An example of obtainable temperature time history is shown in Figure 11 for element ID 9927 (polyurethane element with highest temperature) of wheel type A.

It should be emphasized that the high computational time requested by the proposed full procedure, however, is infinitely smaller than the estimated value for a coupled analysis that simulates the actual contact and rolling state by modeling the whole wheel and associating with the dynamic analysis the coupled thermal analysis.

Conclusions

A fast, reliable and low-cost FE methodology has been developed from a computational point of view, which allows to estimate the increase of the temperature of a generic wheel against the travel on a generic track due to dissipation inside the material without adopt coupled field analysis. It provides the roller coaster designer with a technique that allows to choose which of the available polyurethane wheels sets is best for a given track, that is which shows the lowest increase in temperature and thus the lowest potential damage.

This work is the first step in a wider research activity to determine a law to quantify and cumulate temperature-induced damage in this type of material.

References

Ansys inc., 2012, ANSYS Mechanical APDL Material Reference, release 14.5.

Bakirani, M., Hepburn, C., 1992, Internal Heat Generation and Fatigue Life Behaviour of Polyurethane Elastomer Based on Trans 1,4 – Cyclohexane Diisocinate, Iranian Journal of Polymer Science & Technology, 1(1), 21-24.

Beyler, C.L., Hirschler, M.M., 2008, Thermal Decomposition of Polymers, in SFPE Handbook of Fire Protection Engineering, chapter 1.7, Quincy, Mass.: National Fire Protection Association, Bethesda, Md.: Society of Fire Protection Engineers.

Braccesi, C., Cianetti, F., 2015, Development of a procedure for the structural design of roller coaster structures: The rails, Engineering Structures, 93, 13-26.

Braccesi, C., Cianetti, F., 2018, Development of a procedure for the structural design of roller coaster structures: The supporting structures, Engineering Structures, 168, 643-652.

Brinson, C., Brinson, H., 2008, Polymer Engineering Science and Viscoelasticity. An introduction, Springer – Verlag.

Briody, C., Duigan, B., Jerrams, S., Tierman, J., 2012, The Implementation of a Visco–hyperelastic Numerical Material Model for Simulating the Behaviour of Polymer Foam Materials, Computational Materials Science, 64, 47-51.

Dal, H., Kaliske, M., 2009, Bergström–Boyce Model for Nonlinear Finite Rubber Viscoelasticity: Theoretical Aspects and Algorithmic Treatment for the FE Method, Computational mechanics, 44, 809-823.

de Cazenove, J., Rade, D.A., de Lima, A.M.G., Araújo, C.A., 2012, A numerical and experimental investigation on self-heating effects in viscoelastic dampers, Mechanical Systems and Signal Processing, 27, 433-445.

Ebewele, R. O., 2000, Polymer Science and Technology, CRC Press.

Gogos, C.G., Tadmor, Z., 2006, Principles of Polymer Processing, Wiley–Interscience.

Gopalakrishna, H.S., Lai, M.L., 1998, Finite element heat transfer analysis of viscoelastic damper for wind applications, Journal of Wind Engineering and Industrial Aerodynamics, 77/78, 283-295.

Kalpakjian, S., Schmid, S., 2006, Manufacturing Engineering and Technology, Pearson Education, Inc., Upper Saddle River, NJ.

Mead, J.L., 1996, Mechanical Degradation of a Polyurethane Elastomer, Ph.D. Thesis at the Massachusetts Institute of Technology, Boston, USA.

Paez, T., Piersol, A., 2009, Harris' Shock and Vibration Handbook, McGraw–Hill Professional.

Zeus Industrial Products, 2005, Thermal Degradation of Plastics, Zeus technical whitepaper, www.zeusinc.com.

Zheng, L. H., Liu, Z., Chen, M.L., Zhu, Y.T., 2017, Vibration modeling and position-dependent analysis of spatial trajectory roller coaster, Archive of Applied Mechanics, 87, 489–502.